frontiers in Forests and Global Change

ORIGINAL RESEARCH
published: 12 July 2021
doi: 10.3389/ffgc.2021.689335

Robust Estimation of Absorbing Root Surface Distributions From Xylem Water Isotope Compositions With an Inverse Plant Hydraulic Model

Hannes P. T. De Deurwaerder[1,2], Marco D. Visser[1,3], Félicien Meunier[2], Matteo Detto[1], Pedro Hervé-Fernández[4,5,6], Pascal Boeckx[4] and Hans Verbeeck[2]*

[1] Department of Ecology and Evolutionary Biology, Princeton University, Princeton, NJ, United States, [2] CAVElab–Computational and Applied Vegetation Ecology, Faculty of Bioscience Engineering, Ghent University, Ghent, Belgium, [3] Institute of Environmental Sciences, Leiden University, Leiden, Netherlands, [4] ISOFYS–Isotope Bioscience Laboratory, Faculty of Bioscience Engineering, Ghent University, Ghent, Belgium, [5] School of Environment and Sustainability, Global Institute for Water Security, University of Saskatchewan, Saskatoon, SK, Canada, [6] Facultad de Artes Liberales, Universidad Adolfo Ibáñez, Santiago, Chile

OPEN ACCESS

Edited by:
Yuanyuan Huang, Climate Science Centre, CSIRO Oceans and Atmosphere, Australia

Reviewed by:
Alan Feest, University of Bristol, United Kingdom
Xiaochi Ma, University of California, Davis, United States

***Correspondence:**
Hannes P. T. De Deurwaerder Hannes_de_deurwaerder @hotmail.com

Specialty section:
This article was submitted to Forest Soils, a section of the journal Frontiers in Forests and Global Change

Received: *31 March 2021*
Accepted: *01 June 2021*
Published: *12 July 2021*

Citation:
De Deurwaerder HPT, Visser MD, Meunier F, Detto M, Hervé-Fernández P, Boeckx P and Verbeeck H (2021) Robust Estimation of Absorbing Root Surface Distributions From Xylem Water Isotope Compositions With an Inverse Plant Hydraulic Model. Front. For. Glob. Change 4:689335. doi: 10.3389/ffgc.2021.689335

The vertical distribution of absorbing roots is one of the most influential plant traits determining plant strategy to access below ground resources. Yet little is known of natural variability in root distribution since collecting field data is challenging and labor-intensive. Studying stable water isotope compositions in plants could offer a cost-effective and practical solution to estimate the absorbing root surfaces distribution. However, such an approach requires developing realistic inverse modeling techniques that enable robust estimation of rooting distributions and associated uncertainty from xylem water isotopic composition observations. This study introduces an inverse modeling method that supports the assessment of the root allocation parameter (β) that defines the exponential vertical decay of a plants' absorbing root surfaces distribution with soil depth. The method requires measurements obtained from xylem and soil water isotope composition, soil water potentials, and sap flow velocities when plants' xylem water is sampled at a certain height above the rooting point. In a simulation study, we show that the approach can provide unbiased estimates of β and its associated uncertainty due to measuring errors and unmeasured environmental factors that can impact the xylem water isotopic data. We also recommend improving the accuracy and power of β estimation, highlighting the need for considering accurate soil water potential and sap flow monitoring. Finally, we apply the inverse modeling method to xylem water isotope data of lianas and trees collected in French Guiana. Our work shows that the inverse modeling procedure provides a robust analytical and statistical framework to estimate β. The method accounts for potential bias due to extraction errors and unmeasured environmental factors, which improves the viability of using stable water isotope compositions to estimate the distribution of absorbing root surfaces complementary to the assessment of relative root water uptake profiles.

Keywords: absorbing root surfaces distribution, ecohydrology, lianas, stable water isotopes, tropical trees, water competition

INTRODUCTION

The absorbing root surfaces distribution (A_R), i.e., those surfaces of a plants' root system that support water uptake, is a pivotal plant characteristic that determines the plant species' nutrient and water acquisition strategy. Investments in competitive advantage usually imply maximizing the upper soil layer's exploitation, where the concentration of nutrients is generally highest (Jobbagy and Jackson, 2001). However, this comes at the cost of drought tolerance since upper layers are generally more drought-prone than deeper soil layers with more stable water reserves (Fogel, 1985). Accurate measures of A_R are thus needed to characterize specific plant competitive strength and drought response.

Unfortunately, data on root distributions in general—and on A_R in specific—is scarce, and little is known about the intra- and interspecific variability in A_R across different environments (Böhm, 2012). This paucity is caused in part by the available techniques to study root distributions of individual plants, which are often destructive, expensive, and labor intensive (Cabal et al., 2021). Root excavation, for example, holds the highest promise of most accurately characterizing a plant's natural root distribution (Böhm, 2012). However, the associated workload limits its practical application to small sample sizes and small habitus plants, e.g., annual plants, crops, and young trees. As an illustration, Preston (1942) estimated that one laborer requires approximately 5 weeks to fully excavate and examine the root system of single 15-year-old lodgepole pine. These time and labor disadvantages have led to the development of many other direct and indirect *in situ* techniques, such as rhizotron systems, acoustic and electromagnetic tomography, the auger method, or the use of non-radioactive tracers (reviewed in Cabal et al., 2021). However, while these techniques provide a less invasive alternative to root excavation, they generally fall short in the level of details they can provide on the distribution of the individual absorbing root surfaces.

A relatively straightforward technique to relate relative root water uptake (RWU, which is inextricably linked to A_R) with soil depth is using stable water isotope composition as non-radioactive tracers. Ehleringer and Dawson (1992) described the simplicity of the technique, which lies in a direct relationship between the isotopic composition of the xylem sap (δ_{xyl}) and the isotopic composition observed in soil water (δ_{soil}) along with a soil depth profile. Common approaches assume that xylem water is a proportional mixture of δ_{soil} from the various depths at which roots absorb water (Phillips and Gregg, 2003). The approach requires: (i) the occurrence of a natural isotopic gradient in the soil generated by topsoil water evaporation (Beyer et al., 2018); and (ii) the absence of processes that alter the xylem water isotope composition while entering the plant or during transport along the plant hydraulic system (Wershaw et al., 1966; Zimmermann et al., 1967; White et al., 1985; Dawson and Ehleringer, 1991; Walker and Richardson, 1991; Dawson et al., 2002; Zhao et al., 2016). Requirements (i) and (ii) generally limit the technique to lignified plants and implementation during rain-free periods after sufficient soil evaporation has occurred. However, these conditions still allow strong flexibility and usability across multiple temporal and spatial scales (Dawson et al., 2002). Its moderate labor and time investment allows sampling of more and larger plant species far beyond what is possible with root excavation.

However, the robustness of stable water isotope techniques has been recently questioned (Penna et al., 2018; von Freyberg et al., 2020). An increasing number of studies discuss a potential mismatch between available water sources and isotopically depleted compositions in xylem water. Hypothetical discrepancies have resulted from: isotopic discrimination at root-level (Allison et al., 1983; Vargas et al., 2017) or by associated mycorrhizae (Poca et al., 2019), and by internal mixing of xylem water with isotopically depleted water reserves stored in stem tissue (Barbeta et al., 2020; Knighton et al., 2020). The link between source water and the isotopic composition of xylem water (δ_{xyl}) can be further obscured by pronounced water-transport lags (Meinzer et al., 2006; Gaines et al., 2016; Magh et al., 2020; Marshall et al., 2020; Mennekes et al., 2021) or possible excessive intra-individual variance in δ_{xyl} due to variable RWU dynamics caused by fluctuating biophysical factors, frequently overlooked in isotopic studies (e.g., soil water potentials, vapor pressure deficits and sap flow dynamics) (De Deurwaerder et al., 2020). This growing body of literature suggests that standard sampling methods may deliver biased estimates of RWU profiles while simultaneously underestimating uncertainty among species, biomes, or seasonality. Therefore, a real need exists to develop methods that accurately estimate A_R and associated uncertainty in the face of unmeasured biophysical factors that affect δ_{xyl}.

Coupling stable isotope measurements to biophysical models (e.g., RAPID algorithm) could support the inverse reconstruction of absorbing root surfaces distribution, A_R, and the assessment of their active contribution to RWU (Ogle et al., 2004). Such a coupled technique has enormous potential to build a fundamental understanding of spatial and temporal variability in water competition strategy amongst and within plant species. To the best of our knowledge, only one previous study endeavored to develop such a tool (Ogle et al., 2004). However, it did not account for unmeasured biophysical factors that affect δ_{xyl} potentially leading to biased estimates. Here we adopt a mechanistic model for uptake and transport of stable water composition through plants (De Deurwaerder et al., 2020) and use simulations to show that this inverse modeling method offers estimates of β, the allocation parameter which defines the exponential vertical decay of a plants' A_R while (1) accounting for the xylem water isotopic variance within plants, as well as (2) uncertainties in isotopic measurements and (3) biophysical parameters, e.g., sap flow dynamics. We further provide guidelines to improve sampling design in future studies. Finally, we show how the model can validate previous results by re-analyzing a case study in French Guiana for tree and liana growth forms. This study suggests that previous methods underestimated the uncertainty in mean xylem water δ^2H and $\delta^{18}O$ provided by De Deurwaerder et al. (2018). The applied inverse method is provided as an open-source code (see GitHub repository HannesDeDeurwaerder/iSWIFT).

MATERIALS AND METHODS

The SWIFT model links xylem water isotope compositions (δ_{xyl}) to an allocation parameter β, that defines the exponential vertical decay of A_R with soil depth. We give a brief overview of the model in **box 1**, restricted to key equations expressed for the hydrogen isotope composition in xylem and soil water (δ^2H_X and δ^2H_S). Subsequently, we describe the numerical inversion needed to generate estimates of β from δ_{xyl} and δ_{soil}. Here, we evaluate how increased levels of variable range restrictions improve estimates of β, followed by a power analysis to inform to which extent β should differ between groups of plants subject to similar edaphic conditions to observe statistical differences in δ_{xyl}. Both analyses can help guide future study design optimization. Finally, we introduce a practical case study in French Guiana. We maintain the following notation in the subscripts of presented variables: the medium through which water travels is indicated by uppercase fonts, while lowercase fonts highlight the units of time and distance: *X* for xylem, *R* for root, *S* for soil, *h* for stem height, *t* for time, and *i* for the corresponding soil layer. A complete overview of variables, definitions and units is given in **Supplementary Table 1**, and details on the SWIFT model can be found in **Supplementary Appendix A** and De Deurwaerder et al. (2020).

Inverse SWIFT: Numerical Model Inversion and Likelihood Estimation

The goal is to estimate the relative shape of absorbing root surfaces distribution by numerical inversion of the allocation parameter β, given a set of measured δ_{xyl} collected from plants in the field (**Figure 1**). We start with a vector *C* consisting of paired δ^2H_x and $\delta^{18}O_x$ observations, and assume *C* to be a bi-variate random variable with a conditional probability density function $P(C|\ \beta_{true}, \chi_{true})$ determined by the "true" allocation parameter, β_{true}, and natural occurring variance in the local set of biophysical variables, χ_{true} (**Figure 1A**).

BOX 1 | SWIFT in a nutshell.

SWIFT (Stable Water Isotope Fluctuation within Trees) generates paired predictions of xylem water isotope composition (δ_{xyl}) and the respective sampling error (ξ):

$$\delta_{xyl} = \begin{bmatrix} \delta^2H \\ \delta^{18}O \end{bmatrix} = \begin{bmatrix} f(\beta,\ \chi_{\delta^2H}) \\ f(\beta,\ \chi_{\delta^{18}O}) \end{bmatrix} + \xi \quad \text{(S1)}$$

In SWIFT δ_{xyl} is a function of the relative absorptive root surfaces distribution with soil depth (A_R), determined by allocation parameter β, and a set of biophysical variables (χ) that influence δ_{xyl} other than β (see **Table 1**). We distinguish three distinct groups of biophysical variables in χ:

- ***Physical:*** soil properties, spatial variability in the gradients of soil water isotope composition (δ_{Soil}), and in the soil water potential (Ψ_S) with soil depth, hereafter indicated as soil heterogeneity.
- ***Biological:*** plant trait, i.e., the sapwood area ($A_{SAPWOOD}$), the lumen fraction (*LF*), the effective root radial conductivity (k_R) and the sap flow dynamics (*SF*).
- ***Sampling:*** sampling strategy related variables, i.e., the height (*hos*) and time (*t*) of the day during sampling.

The biophysical variables are the same for both water isotopes ($\chi_{\delta^{18}O}$ and χ_{δ^2H}) except for the isotopic soil profiles (δ_{Soil}; δ^2H_S & $\delta^{18}O_S$). The error term ξ includes cryogenic water extraction errors, since these errors unavoidably occur during the extraction procedure (Orlowski et al., 2013). The magnitude of these errors are within the conservative range of 3 and 0.3‰ for δ^2H and $\delta^{18}O$, respectively (Araguás-Araguás et al., 1995). In the Monte Carlo method these errors are simulated as independent Gaussian random variables to generate δ_{xyl} values.

Relation between A_R and β. The discrete representation of A_R is a function of the total absorbing root area available to the focal plant (A_{Rtot}) allocated via parameter β over all soil depths, z_i (cm), discretized in layers of thickness Δz as follows (Jackson et al., 1996):

$$A_R = A_{Rtot} \cdot \beta^{z_i} \cdot (1 - \beta^{\Delta z}) \quad \text{(S2)}$$

Key mechanics. SWIFT couples (i) a standard multi-source mixing model approach (Phillips and Gregg, 2003) which composes the weighted isotope composition entering the stem base of a plant of the relative quantities of water taken up and the respective δ_{soil} at each soil layer (*i* = 1,2,..,n), with (ii) a mechanistic plant hydraulic module to simulate the impact of root water uptake (RWU) and xylem transport dynamics on δ_{xyl}.

The deuterium isotope composition of water entering the stem base of a plant ($\delta^2H_{X,0,t}$) at time *t* is a weighted sum of the product of the relative water taken up ($F_{i,t}$) from each layer and the corresponding $\delta^2H_{S,i}$. Assuming soil conductivity is much bigger than k_R, a simplified model for the $\delta^2H_{X,0,t}$ can be given as (for a complete formulation that includes soil and root conductivity, see **Supplementary Appendix A**):

$$\delta^2H_{X,0,t} = \sum_{i=1}^{n} F_{i,t} \cdot \delta^2H_{S,i} = \sum_{i=1}^{n} \frac{\beta^{z_i} \cdot \Delta\psi_{i,t}}{\sum_{i=1}^{n} \beta^{z_i} \cdot \Delta\psi_{i,t}} \cdot \delta^2H_{s,i} \quad \text{(S3)}$$

$F_{i,t}$ depends on (i) the relative amount of absorbing root surface per soil layer available to the plant (β^{z_i}), and (ii) the ability of these root surfaces to uptake water based on the water potential gradient between root xylem and soil ($\Delta\Psi_{i,t}$). In the present model, root water potentials show diurnal variability driven by plant responses to fluctuating abiotic conditions (i.e., vapor pressure deficit). The latter leads to a variable $\delta^2H_{X,0,t}$ which then propagates along the stem of the plant, causing a lag between the isotope compositions entering the plant and that of extracted δ_{xyl} samples taken at different heights. SWIFT takes this into account by computing the time, τ, a molecule of ^2H takes to travel from where it was extracted, $\delta^2H_{X,0,t}$, to the height *h* where samples were taken, $\delta^2H_{X,h,\ t}$, using modeled or observed sap flow velocities.

Merits of using SWIFT. The SWIFT implementation considers that variance in the χ variables can indeed (i) transmit in differences in a plant's root water uptake ability and rates at different soil layers (i.e., Ψ_S, $\delta^2H_{S,i}$, k_R and *SF*) which causes variance independent of β, and (ii) account for transportation lag and optimized sampling (i.e., $A_{SAPWOOD}$, *LF*, *SF*, *hos*, and *t*). Both (i) and (ii) are generally disregarded in stable water isotope studies, leading to potential biases in derived insights from δ_{xyl} samples, hence in RWU and β.

TABLE 1 | Overview of the variable restrictions (X: restricted; o: non-restricted) considered within the inverse SWIFT procedure to simulate synthetic field data and corresponding conditional density probability distributions $P(\delta_{xyl}|\beta, \chi)$.

Abbr.	Description	Field data	Sc.A	Sc.B	Sc.C	Sc.D
$A_{SAPWOOD}$	Sapwood area	**X**	o	o	o	**X**
δ^2H_S	Soil water isotopic signature defined per soil depth	**X**	o	**X**	**X**	**X**
hos	Height of sampling	**X**	o	o	**X**	**X**
k_R	Effective root radial conductivity	**X**	o	o	o	**X**
L*F*	Lumen fraction per unit sapwood area	**X**	o	o	o	**X**
SF	Instantaneous sap flow at time *t* corrected based on DBH of each individual	**X**	o	o	o	**X**
t	Time of sampling during the day	**X**	o	o	**X**	**X**
Ψ_S	Water potential at a specific soil layer depth *i* and time	**X**	o	**X**	**X**	**X**
β	The allocation parameter which defines the shape of exponential vertical decay of the distribution of absorbing root surface distribution with soil depth.	0.966	$\beta_{[i]}$	$\beta_{[i]}$	$\beta_{[i]}$	$\beta_{[i]}$
Rest. Group	Variable restriction group considered per scenario	Physical Sampling Biological	o	Physical	Physical Sampling	Physical Sampling Biological

The distinct scenarios (Sc.) represent different levels of prior knowledge of the parameter set χ*. Sc. A: No restrictions are considered. Sc. B: Restriction imposed on the physical variables, i.e., the soil heterogeneity. Sc. C: Restriction of both the physical variables and the sampling strategy. Sc. D: Full restriction, thus considering an additional restriction on the biological plant-specific variables. More details in the main text, and the precise applied parameter restriction ranges for each scenario are provided in* ***Supplementary Table 2*** *and* ***Table 1****.*

Subsequently, we consider Equations 1–3 (**Box 1**) to generate distributions of synthetic δ_{xyl} values that correspond to a wide range of biophysical parameters (χ) which prior distributions are user-specified or measured (**Supplementary Table 2**) and given a specific value of β (**Figure 1B**). These distributions are defined as conditional probability density distributions where $P(\delta_{xyl}|\beta, \chi)$ represents the range of possible δ_{xyl} values generated by the SWIFT model (hereafter "Synthetic δ_{xyl}"), given a specific β and uncertainty in χ. We then vary the parameter β, generating new distributions associated with each considered β-value, $P(\delta_{xyl}|\beta, \chi)$, until we find the distribution that maximizes the likelihood of observing the field samples *C* (**Figure 1C**). This maximum likelihood estimate of β (hereafter indicated as $\widehat{\beta}$) is then assumed to be the best approximation of β_{true}. The distribution of each biophysical variable in χ can be based on prior measurements of the studied system or set as uninformative uniform distributions when no prior knowledge is available. A schematic workflow of this Inverse SWIFT approach is provided in **Figure 1**.

Likelihood and Model Optimization

The inversion procedure starts by numerically generating a vector of paired $\begin{bmatrix} \delta^2 H \\ \delta^{18} O \end{bmatrix}$ values (see Equation S1) for a given value of β, with other parameters drawn by *q* Monte-Carlo simulations from the user assigned or measured distributions of each biophysical variable χ. Here, we set *q* to 250, and the distributions of χ are given in **Supplementary Table 2**. The conditional density probability distributions $P(\delta_{xyl}|\beta, \chi)$ are computed using a bivariate kernel density estimator (i.e., the *kde* function of the *"ks"* R-package, Duong, 2007). The likelihood of observing *C*, the paired δ_{xyl} values from field data of *k* samples (j = 1, 2, . . ., k), is then defined as:

$$\mathcal{L}(\beta \mid C, \chi) = \prod_{j=1}^{k} \mathrm{P}\left(C_j \mid \beta, \chi\right) \quad (1)$$

The β of the $P(\delta_{xyl}|\beta, \chi)$ which minimizes the sum of the negative log-likelihood function, given the observed *C,* is then considered as the best estimate of β_{true}, i.e., $\widehat{\beta}$.

$$\widehat{\beta} \in \mathrm{argmin}\left\{ -log\mathcal{L}(\beta|C, \chi)\right\} \quad (2)$$

The search of β values is restricted to the range 0.905–0.995, according to the global analysis in Jackson et al. (1996). A one-dimensional general-purpose optimization method was used to find minima for Equation 2 (*"brent"* method in the *"stats"* package *optim* function, R Core Team, 2017).

Bias Evaluation in the Inversion Procedure

To quantify how the three distinct parameter sets defined earlier–physical, biological, and sampling (**Box 1**)–influence the likelihood, bias, and power, we generated sets of synthetic δ_{xyl} data (C_{SYN}) with known values of β (β_{true} and χ_{true}; β_{true} set at 0.966. The selected value is representative for temperate deciduous forest rooting profiles after Jackson et al. (1996; see **Table 1** and **Supplementary Table 2**) and then inversely estimated $\widehat{\beta}$ and associated likelihood profiles. During this procedure, the following four scenarios of increasing variable restriction of χ are considered and represent different levels of prior knowledge on the parameter set χ.

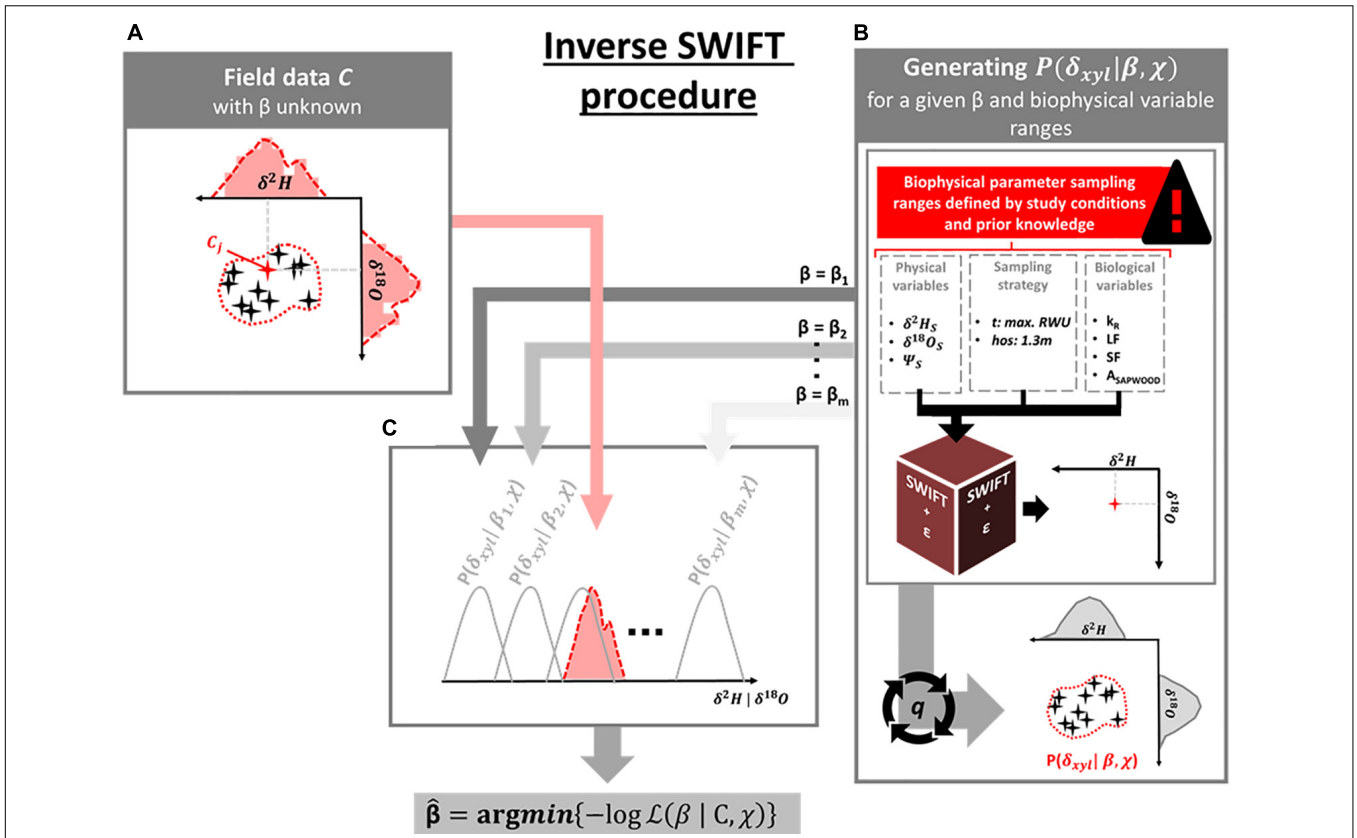

FIGURE 1 | Schematic overview of the Inverse SWIFT procedure which supports estimation of the plant groups' mean allocation parameter β (which defines the exponential vertical decay of the distribution of absorbing root surface with soil depth) from the respective xylem water isotopic compositions [(δ_{xyl}; being δ^2H and/or $\delta^{18}O$, subplot **(A)**]. Specifically, a model that couples a standard multi-source mixing model with a mechanistic plant hydraulic model, e.g., the SWIFT model, allows for the generation of theoretical xylem water isotopic field data for a given β and a set of biophysical model variables (χ) **(B)**. In this way, conditional density probability distributions ($P(\delta_{xyl}|\beta, \chi)$) are established for a range of β-values to which field data *C* can be matched **(C)**. The β-value which correspond to the ($P(\delta_{xyl}|\beta, \chi)$) which minimizes the log-likelihood function provides the best β-estimate ($\hat{\beta}$) of the studied plant group.

Scenario **A: No variable range restrictions.** This scenario assumes no prior knowledge of the system, except for δ_{Soil} and soil water potential (Ψ_S) profiles with soil depth. This corresponds to the most common study conditions (Rothfuss and Javaux, 2017). Ideally, well-characterized δ_{Soil}-profiles from homogeneous soils yield the best results but in natural settings, soil heterogeneity can lead to high spatial variability which causes large random sampling errors. Therefore, we start from clearly defined empirical $\delta^{18}O_S$ and Ψ_S profiles, hereafter the "true profiles" (illustrated by those obtained by Meißner et al. (2012)) and sample more uncertain "observed" soils profiles (using ± 3 standard deviation from the true $\delta^{18}O_S$ and Ψ_S, profiles see functions **Supplementary Table 2**)—hereafter "heterogeneous profiles." As we assume equilibrium conditions δ^2H_S profiles are deduced from $\delta^{18}O_S$ using the local meteoric water line (LMWL) (for details see **Supplementary Appendix B**).

Scenario **B: Variable range restriction of the soil heterogeneity.** Here the Ψ_S and δ_{Soil}-profiles are assumed to be characterized with higher precision. The input parameterization now considers narrow variance ranges, i.e., mean ± 1 standard deviation of the Ψ_S and $\delta^{18}O_S$ true profiles. Yet again, δ^2H_S profiles are calculated from $\delta^{18}O_S$ using the LMWL.

Scenario **C: Variable range restriction by sampling strategy.** Restricting sampling of δ_{xyl}–values to periods that correspond to maximum RWU activity may decrease bias (see De Deurwaerder et al., 2020). In this scenario, we assumed that the sampling strategy was optimized in timing (*t*) and the height of sampling (*hos*) targeting representative δ_{xyl} values representative for peak RWU. Specifically, the height of sampling is set at 1.3 m, which corresponds to the general practice of sampling trees at breast height. Subsequently, we define the sampling time by the moment the δ_{xyl}–values that correspond to the plant's peak water uptake of the plant passes the 1.3 m sampling height, which depends on the plant's sap flow velocity.

Scenario **D: Variable range restriction of biophysical plant traits.** Knowledge of natural variance in plant-specific input variables can be used to restrict the model. In practice this can be done via direct *in situ* measurement or through literature information. In this scenario, we consider the sapwood area ($A_{SAPWOOD}$), the lumen fraction (*LF*), the effective root radial

conductivity (k_R) and the instantaneous sap flow (SF) known to a much better degree allowing restriction of their range and distribution (provided in **Table 1** and **Supplementary Table 2**).

Bias in the $\widehat{\beta}$ was calculated as $\frac{\beta_{true}-\widehat{\beta}}{\beta_{true}}$. We calculated the bias for different sample sizes (C_{SYN} with 5, 25 and 50 samples) and all scenarios. Per scenario and sample size, we randomly assign a β_{true}, inversely estimate $\widehat{\beta}$ and calculate bias for 500 independent simulations per scenario (with $q = 250$). The latter reveals which combination of sample size and set of variable restrictions (physical, biological, or sampling) yields the largest considerable estimation accuracy improvement.

Power Analysis

A power analysis quantifies the ability to distinguish between plant groups with different relative A_{R-}profiles (as determined by β). Here we generate two sets of synthetic δ_{xyl} values which correspond to distinct plant groups which have similar χ, but differ in β. By inverse modeling, we computed the corresponding $\widehat{\beta}_1$ and $\widehat{\beta}_2$ via the inverse model approach as it would be done in actual study conditions. The power analysis consists of two parts. First, we quantified the minimal detectable difference (d), being the smallest statistical detectable difference between groups for each scenario. Here, d is the difference in $\widehat{\beta}_1$ and $\widehat{\beta}_2$where the mean of one conditional density probability distributions $P(\delta_{xyl}|\beta, \chi)$ is outside the 95% quantile of the other. Hence, we generated $P(\delta_{xyl}|\widehat{\beta}_1, \chi)$ and $P(\delta_{xyl}|\widehat{\beta}_2, \chi)$ for each scenario as described above (see section "Likelihood and Model Optimization"). Secondly, we calculated how often a significant difference would be detected for a different combination of β values under each scenario. We maintained the standard power level of 0.80 as a validation level for different sample sizes (i.e., 5, 25, and 50).

Case Study: Estimation of the Generic Rooting Depths for Trees and Lianas in French Guiana

In the case study, we examine two growth forms, lianas and trees, that strongly differ in traits that could bias RWU depth estimation, i.e., hydraulic properties and sap flow dynamics (Chen et al., 2015). We also evaluate differences in sampling strategy where a standard approach is compared to a setup where Ψ_S profiles were measured in Laussat, French Guiana, in 2017 (**Supplementary Figures 3, 4**). The two setups allow us to quantify the impact of different degrees of parameter restriction in the inverse model procedure.

Sampling Strategy Field Data

Setup A applies a standard setup that ignores soil properties, e.g., Ψ_S profile, and plant physiological processes that increase variance in δ_{xyl}. The latter is similar to the sampling strategy applied in De Deurwaerder et al. (2018). This standard method ignores uncertainty in the biophysical variables and uncertainty introduced by sampling. For instance, stem cores were taken at breast height for trees, while for lianas, sampling was done at various heights, which depended on branch accessibility for the climber. Sampling at different heights requires correction for the expected lag in transport (see **Box 1**), and not correcting for sampling height can lead to underestimation of uncertainty (De Deurwaerder et al., 2020). Here, insights in sap flow velocities and related biophysical variables (i.e., lumen area and root radial conductivity) would govern insights in daily variance in plant water potentials. The latter drives RWU dynamics, hence the incoming mixture of isotope compositions of tapped soil water sources. Such sap flow measurements would also support the characterization of the transportation lag essential for correctly matching δ_{xyl} with the driving abiotic conditions at the time of uptake. Hence, we expect that ignoring unmeasured biophysical variables and the sampling design can lead to an underestimation of the error in mean δ_{xyl} compared to using the inverse SWIFT method.

Setup B differs from A in that representative Ψ_S profiles were obtained from soil water potential sensors installed at the Paracou field station (French Guiana, period 15/09-15/10 2017, 3 setups of MPS-6 dielectric water potential sensors, Decagon Devices, Inc. Washington, United States). Given its similarities in edaphic and environmental conditions, the *in situ* Ψ_S monitored in Paracou is considered representative for the Laussat study site. Pooling all the data per monitoring depth (i.e., 15, 30, 45, 60, and 90 cm) provided Ψ_S averages and variance, allowing the construction of a representative Ψ_S profile for inverse SWIFT.

For both setups A and B, we estimated the uncertainty in mean δ_{xyl} values, tested whether significant differences were observed between lianas and trees which informs RWU depth and evaluated the influence of improved monitoring to restrict the unknown parameter space of our inverse model. In line with De Deurwaerder et al. (2018), we assume more inter- than intra growth form differences in rooting distributions. All samples were therefore clustered according to their growth form, and model parameterization was guided by growth form specific empirical data from literature. Further details on the study site, sampling strategy and extraction protocols are provided in **Supplementary Appendix C**.

Applying the Inverse Model

In both case study setups, we consider a moderately constrained version where various biophysical SWIFT input variables are obtained by reasoned assumptions from literature and measurements collected under similar conditions (**Supplementary Table 3**). In **Supplementary Appendices B–D**, we supply descriptions of the dual-isotope plots (**Supplementary Figures 3, 4**), applied data collection and processing which account for the observed δ^2H offset (after Barbeta et al., 2019), as well as detailed information concerning datasets used for inverse SWIFT parameterization of both setups (**Supplementary Table 3**). This case study is restricted to clay plots as no representative Ψ_S data is available for sand plots needed to enable qualitative assessment of β. The lack of a Ψ_S profile obscures the link between absorbing root surfaces distribution and the water uptake activity and rates per soil layer, hence imposing a bias in $\widehat{\beta}$ which we are unable to quantify. Finally, the inverse SWIFT approach was performed for 10 independent iterations to quantify bias, where the average of all iterations represents the generic $\widehat{\beta}$ of the studied liana and tree communities.

RESULTS

Model Simulation With Synthetic Field Data

The minima of log-likelihood profiles for each simulation showed a $\widehat{\beta}$ close to β_{true}. Robust and unbiased $\widehat{\beta}$ will require some restrictions in the variable ranges and measurement uncertainty. In most cases, simulations show that log-likelihood curves tend to be flatter when little restrictions were applied (**Figures 2**, **3** and **Supplementary Figure 2**), implying significant uncertainty. The log-likelihood curves were generally steeper when soil heterogeneity (Sc. B) and an optimized sampling strategy (Sc. C) were considered. Interestingly, an increase in sample size had only a moderate effect on decreasing uncertainty (**Figure 3**) compared to applying other restrictions (**Figures 2**, **3** and **Supplementary Figure 2**), indicating that effort in reducing uncertainty in biophysical variables should be a priority. Bias was greatest with no variable range restrictions (scenario A), resulting in underestimation compared to β_{true} (**Figure 3**), since the generated $P(\delta_{xyl}|\beta, \chi)$ were skewed to more negative signatures (**Figure 4B**). The peak of $P(\delta_{xyl}|\beta, \chi)$ narrows with increased scenario restrictions resulting in an improved ability to distinguish different datasets (**Figure 4**). Restriction of the soil heterogeneity reduced the width of $P(\delta_{xyl}|\beta, \chi)$, albeit a distinct tail toward more depleted isotope compositions remained (**Figure 4B**). An optimized sampling strategy overcame this skewness (**Figure 4C**) and hence provided an improved $\widehat{\beta}$ which was no longer biased toward overestimation. As expected, the greatest restriction of the biophysical plant variables (Sc. D) yielded the lowest bias, although improvements from scenario C were modest (**Figures 2–4**).

The power analysis showed that the minimal detectable difference in β-values increased as plants became shallower rooted (**Figure 5**, see example in panel C), allocating most of their absorbing root surface in the upper soil layers (i.e., when β of the focal plant is lower). A larger difference in β, or more variable range restrictions, will be needed when studying shallow-rooted plants. A significant difference in the average δ_{xyl} can be detected earlier when plants are more deeply rooted (larger β). In all cases, increased sample size resulted in additional power, but the greatest improvement was obtained by restricting the parameter space with prior knowledge, measurements, or study design (**Figure 5**).

Practical Case Study

We observed a shallower shape of the absorbing root surfaces distribution, i.e., smaller $\widehat{\beta}$, for lianas (0.657, i.e., half of A_R in the upper 2 cm soil layer) than for their co-occurring trees (0.954, i.e., half of A_R in the upper 15 cm soil layer) (**Figure 6**; parameterization **Supplementary Table 3**). However, as setup A ignored all biophysical parameters, uncertainty in the estimates is much larger and showed a non-robust difference between lianas and trees (**Figure 6A** and **Table 2**). This considerable uncertainty resulted from the poor characterization of Ψ_S profile. Applying inverse SWIFT for scenario B, with field measurements of the Ψ_S, resulted in a much more conspicuously difference in mean δ^2H for trees and lianas and a substantial reduction in uncertainty, i.e., an uncertainty range improvement of $\sim$ 4.0 (**Figure 6** and

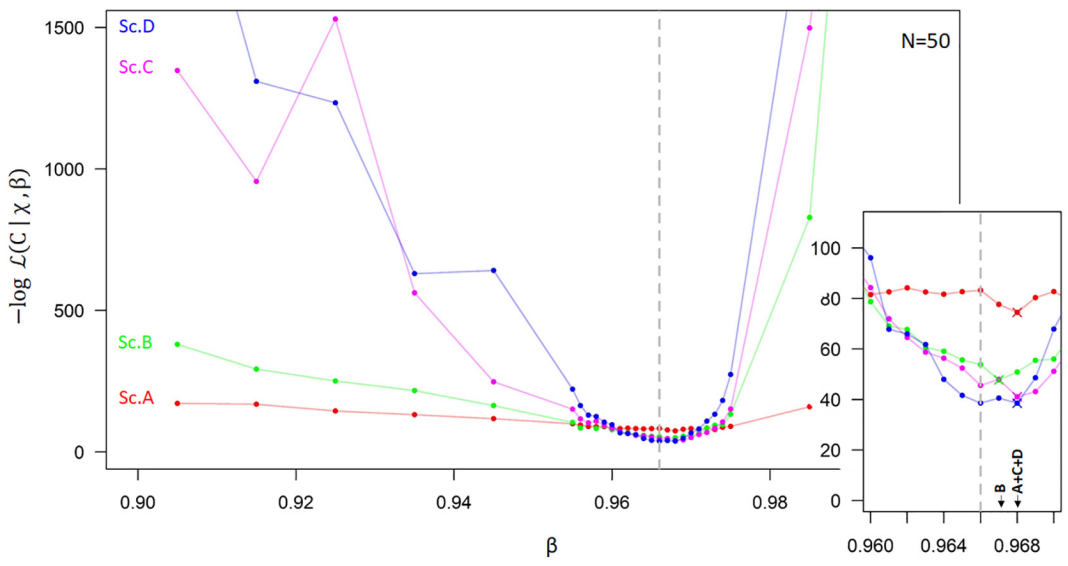

FIGURE 2 | Example of a Log-likelihood curve (–log $\mathcal{L}(\beta|C, \chi)$) as a function of the allocation parameter β which defines the exponential vertical decay of the distribution of absorbing root surface with soil depth, under four different scenarios (Sc. A–D). The best β estimate ($\widehat{\beta}$), has the minimal log-likelihood values shown for each scenario in a magnified panel (the true β is indicated by the dashed line, β_{true} = 0.966). This figure represents a sample size (*N*) of 50 individuals. **Supplementary Figures 2A,B** shows similar likelihood profiles for smaller sample sizes. Sc. A: No restrictions are considered. Sc. B: Restriction imposed on the physical variables, i.e., the soil heterogeneity. Sc. C: Restriction of both the physical variables and the sampling strategy. Sc. D: Full restriction, thus considering an additional restriction on the biological plant-specific variables. More details in the main text and the applied parameter restriction for each scenario are given in **Supplementary Table 2** and **Table 1**.

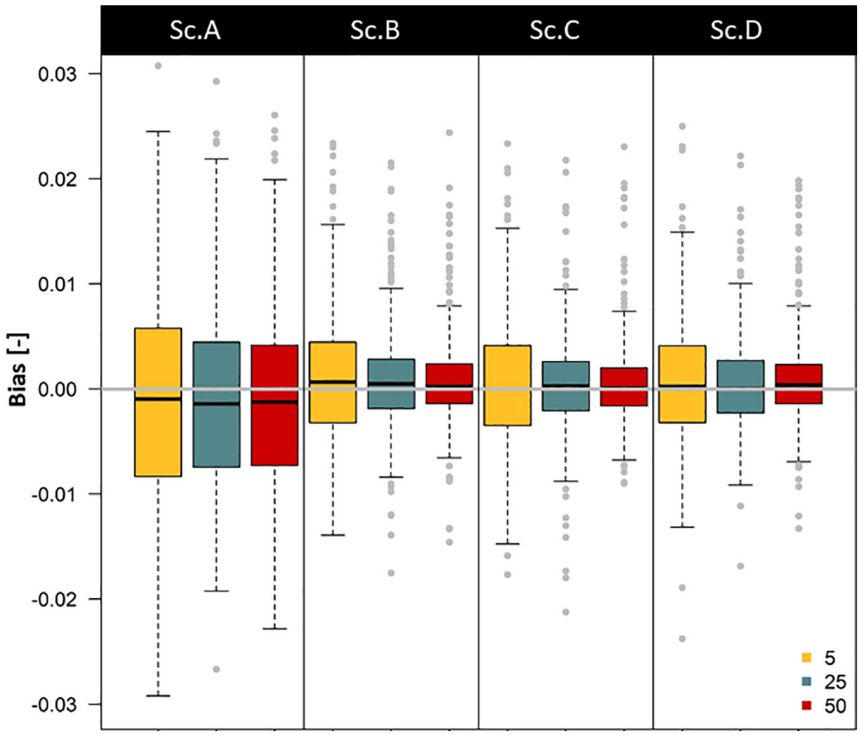

FIGURE 3 | Boxplots showing the expected bias in β estimation ($\widehat{\beta}$) for four theoretical scenarios, bias decreases when key biophysical parameters (χ) are known or when the sample size increases. Sc. A: No variable range restrictions are considered. Sc. B: Restriction imposed on the physical variables, i.e., the soil heterogeneity. Sc. C: Restriction of both the physical variables and the sampling strategy. Sc. D: Full restriction, thus considering an additional restriction on the biological plant-specific variables. Different boxplots' colors show the considered sample size (5: yellow, 25: blue, 50: red). Boxplots show Q25 - 1.5 IQR, Q25, Q50, Q75 and Q75 + 1.5 IQR values, with IQR the interquartile range. Outliers are provided as gray dots.

Table 2). The latter highlights the uncertainty underestimation by De Deurwaerder et al. (2018), which used a standard approach due to unmeasured biophysical parameters.

DISCUSSION

This study introduces a parametric method to estimate A_R with stable isotope data. The main benefit of the inverse SWIFT approach is that it provides a more realistic quantification of uncertainty, as well as improved accuracy (**Figure 3**). Simulations suggest that $\widehat{\beta}$ will likely be systematically overestimated and uncertainty considerably underestimated when ignoring field conditions. Both uncertainty and estimation bias can be significantly reduced by (1) improved characterization of soil heterogeneity (i.e., by accurate characterization of Ψ_S and δ_{Soil}) in combination with (2) optimized sampling that accounts for RWU and sap flow dynamics (De Deurwaerder et al., 2020). The former implies a study setup that monitors δ_{Soil} and Ψ_S in different soil layers and locations, and our simulation suggest that this should be prioritized above increasing the number of δ_{xyl} samples. The latter involves the application of a study design where sampling targets the δ_{xyl} corresponding to peak RWU, which results in a more pronounced V-shaped log-likelihood curve (**Figure 2**), i.e., less skewness in $P(\delta_{xyl}|\beta, \chi)$ and hence far less uncertainty.

Case Study Findings

De Deurwaerder et al. (2018) reported significantly enriched δ_{xyl} for lianas compared to co-occurring trees during the dry season in Paracou (French Guiana) which suggests shallower root systems for lianas (as also shown elsewhere: Johnson et al., 2013; Carvalho et al., 2016; Smith-Martin et al., 2019, 2020). However, De Deurwaerder et al. (2018) approach ignored soil properties and many plant physiological processes that increase variance in δ_{xyl}. As our case study for Laussat shows, the lack of relevant biophysical information results in underestimating uncertainty in the mean δ_{xyl}. The latter implies that the findings of De Deurwaerder et al. (2018) can be explained by factors other than rooting depth, and should in hindsight have been interpreted with more caution than initially reported. Next, we applied an improved sampling setup in Laussat with a better representation of Ψ_S, which resulted in a strong drop in uncertainty and while still suggesting that a shallower absorbing root surface distribution for lianas is required to explain the differences in δ_{xyl} at least when only considering the confounders included in the current model (see "Recommendations and Future Directions" below). The results of these case study are also in line with our power analysis (**Figure 5**), which show that better quantification of Ψ_S should yield an improved ability to detect robust differences between these two growth forms. This highlights the importance of optimizing data collection and sampling strategy.

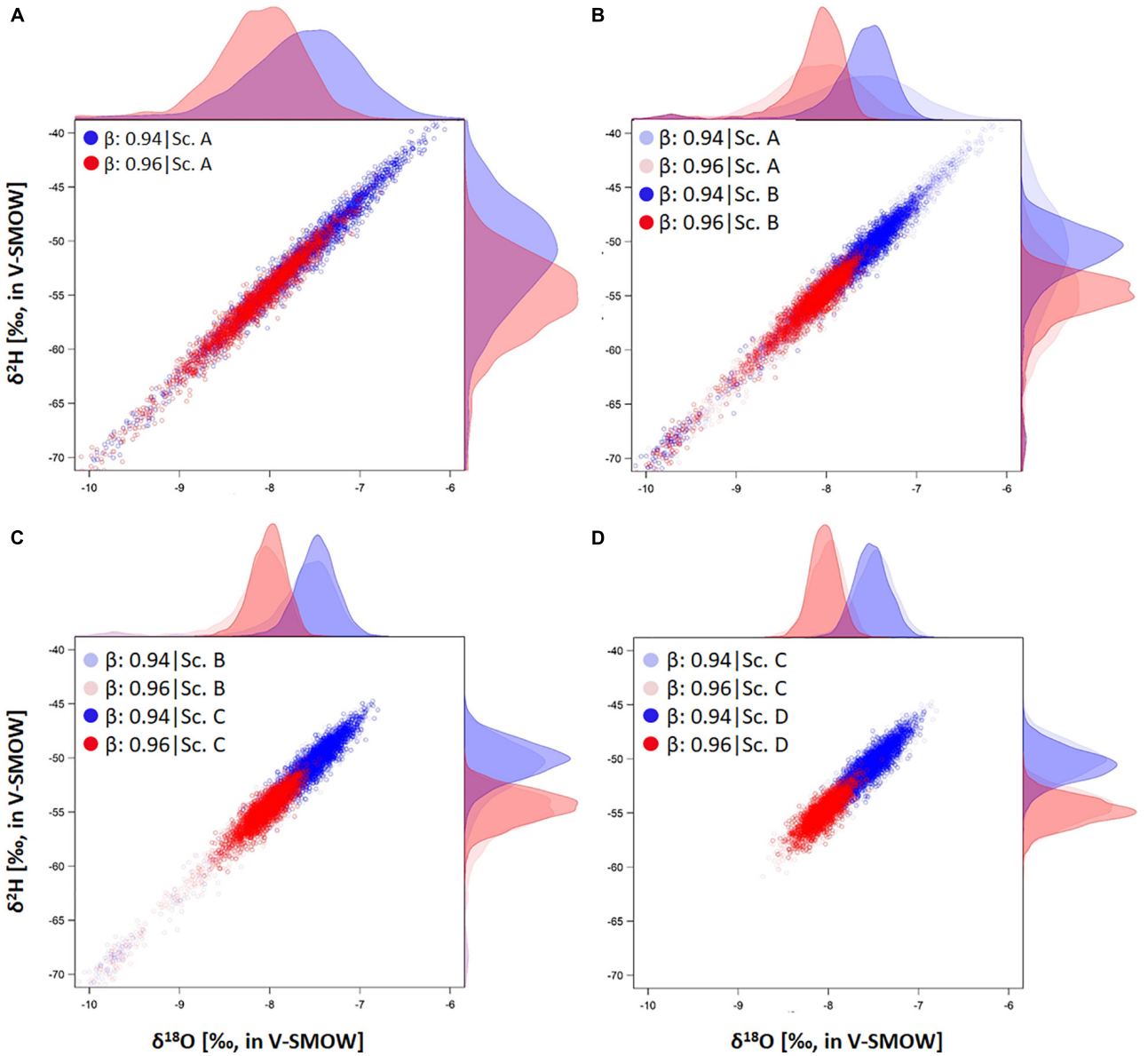

FIGURE 4 | Representation of the simulated conditional probability distribution [i.e., $P(\delta_{xyl}|\beta, \chi)$] of xylem water isotope composition (δ_{xyl}) with two distinct profiles in absorbing root surface distribution, i.e., β = 0.94 (•) and β = 0.96 (•). Each point represents an individual δ_{xyl} sample generated by the SWIFT model. Different panels **(A–D)** show the results for $P(\delta_{xyl}|\beta, \chi)$ under different theoretical scenarios - Sc. A: No variable range restrictions are considered. Sc. B: Restriction imposed on the physical variables, i.e., the soil heterogeneity. Sc. C: Restriction of both the physical variables and the sampling strategy. Sc. D: Full restriction, thus considering an additional restriction on the biological plant-specific variables. Shaded colored probability distributions in panel **(B–D)** enable comparison with the $P(\delta_{xyl}|\beta, \chi)$ results of the preceding scenario output. $P(\delta_{xyl}|\beta, \chi)$ per isotope composition, i.e., δ^2H and $\delta^{18}O$, are displayed on the panel sides in the respective color of their β.

Recommendations and Future Directions

De Deurwaerder et al. (2020) showed that many biophysical variables could contribute to the intra-individual variance in δ_{xyl}. In the present study, we discussed how a power-analysis using mechanistic plant hydrological models could help optimize study designs and help restrict confounding parameters by identifying the most important biophysical variables to monitor. The latter could be invaluable to optimize sample sizes to maximize the efficient use of labor, resources, and time. Our simulations and analysis suggest that monitoring of soil heterogeneity (i.e., Ψ_S, $\delta^{18}O_S$, and δ^2H_S profiles) and sap flow dynamics contribute to increased power in the detection of differences between plants in their distribution of absorbing root surfaces (A_R), especially when targeted sample sizes are small.

The use of stable water isotopes offers a scalable, time and labor efficient alternative for root excavation. When this is combined with models such as inverse SWIFT,

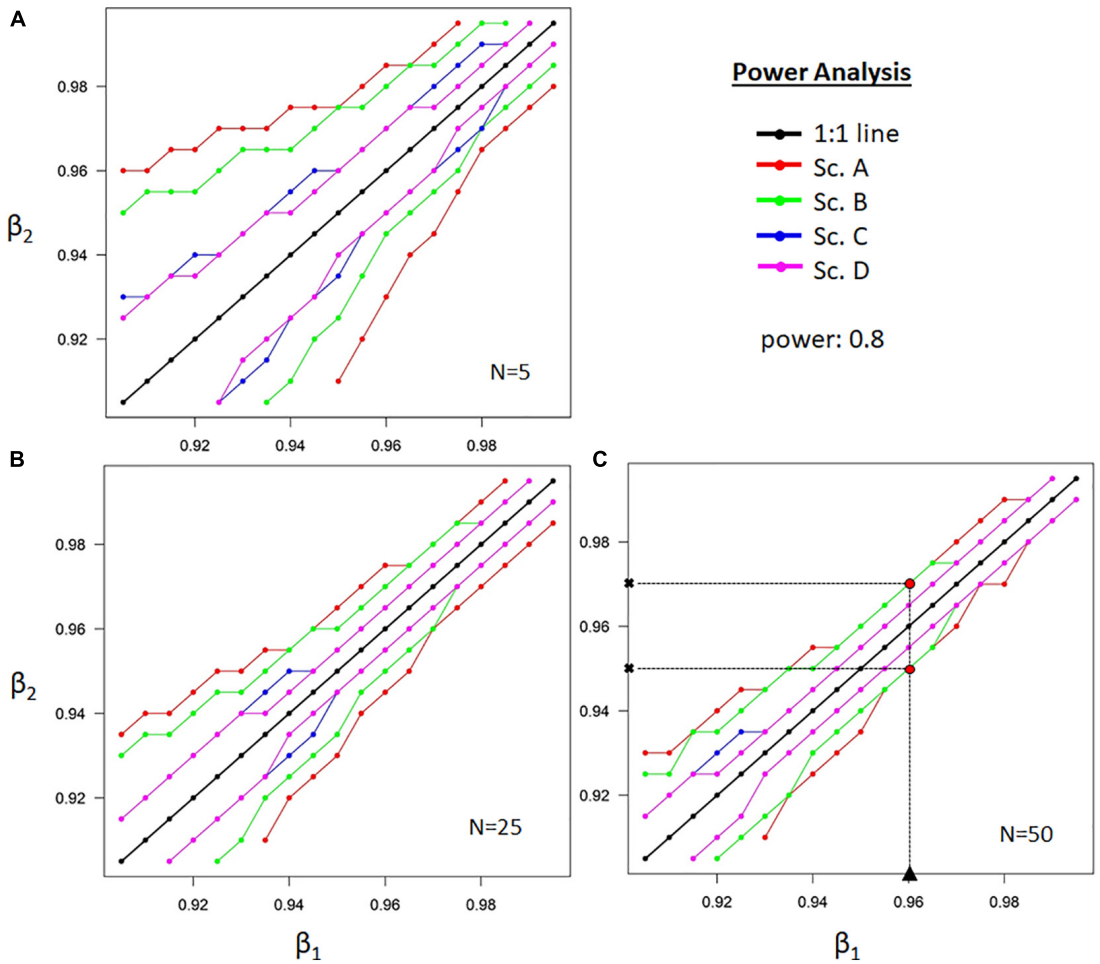

FIGURE 5 | The power analysis shows the combinations of two allocation parameters that define the exponential vertical decay of the distribution of absorbing root surface with soil depth (β) of two independent datasets for a given sample size *N*, required to detect significant differences. Regions bounded by lines are non-significant (at the 95% level). The different colors correspond to four scenarios, as described in the main text and **Figure 2**. Panel **(A–C)**, respectively show power analysis for sample sizes of 5, 25, and 50 samples. The level of confidence of finding significant differences, i.e., the power, is set at 0.8. An example is provided in **(C)** for a study case with $\beta_1 = 0.96$, $N = 50$ and no restrictions (Sc A.). Significant differences can be expected with a power of 0.8 when the compared species has β-values outside the delineated range of both obtained β_2-values.

we show that the A_R (as defined by β) can be assessed indirectly with high accuracy and power. This technique is not only unique in its ability to simultaneously assess A_R and RWU; but its less intrusive nature also supports repetitive sampling to study temporal dynamics. However, intra-individual variance in δ_{xyl} may be impacted by physiological plant processes or soil properties currently not considered. The robustness of the inverse approaches such as the one used here might therefore benefit from further improvements. The latter will require applying both (i) a more realistic modeling and improved theory; and (ii) more experimental and empirical work that monitors the impact of relevant physiological plant processes or soil properties on variance in δ_{xyl}. Essential considerations include temporal and spatial soil dynamics, fractionation at the root level, and storage tissue and phloem enrichment (see also De Deurwaerder et al., 2020).

Inverse SWIFT provides a robust tool to estimate β for plants which A_R approximates a power-law distribution. The latter is a basic representation of root systems in the current SWIFT model. A promising starting point for improvement would be the representation of roots to include more details as in models such as R-SWMS (Javaux et al., 2008) or SPACSYS (Wu et al., 2007). Such detail may be required to account for temporal and spatial soil and root dynamics properly, and in extension their impact on δ_{xyl}. Moreover, such approaches would support an improved representation of the flow path length within the rooting system allowing a more realistic propagation of isotopic composition from soil to the stem base (Seeger and Weiler, 2021).

The implementation of mycorrhizal colonization as an integral component of the water uptake process may present an additional perspective for future model improvement. While their direct contribution to RWU remains unclear (Ruth et al., 2011), various studies have highlighted an increased

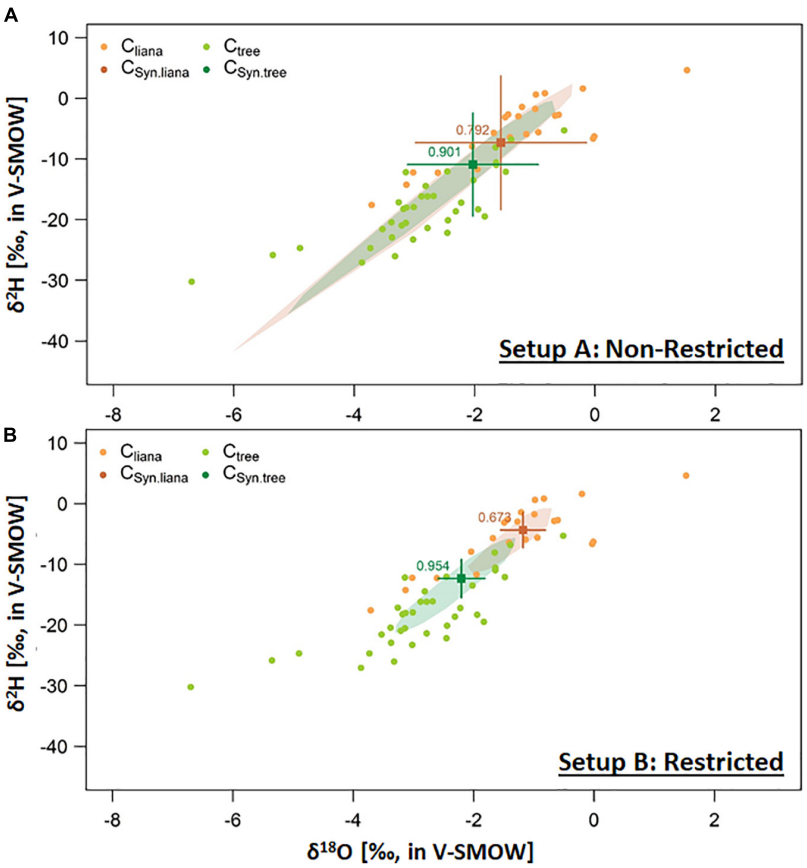

FIGURE 6 | Dual isotope plot representation of the xylem water isotope compositions (δ_{xyl}) of trees (C_{tree},●) and lianas (C_{liana},●) obtained in Laussat, French Guiana, in 2017. **Setup (A)** Study setup which ignored restriction in soil water potential measurements, i.e., Ψ_S and **Setup (B)** Study setup with a more superior characterization of Ψ_S. Mean ± 2x standard error of simulated δ_{xyl} provided for the mean $\widehat{\beta}$ of 10 independent optimization assessments (i.e., $P(\delta_{xyl}|\widehat{\beta}, \chi)$), provided for trees ($C_{Syn.tree}$, ┼) and lianas ($C_{Syn.liana}$, ┼). Corresponding convex hulls shows the pooled simulated δ_{xyl} range for all 10 independent optimizations. Applied parameterization is provided in **Supplementary Table 3**. Mean optimized $\widehat{\beta}$ values are provided in respective colors. Related standard error confidence intervals are provided in **Table 2**.

root hydraulic conductivity because of mycorrhizal colonization (Gianinazzi-Pearson and Gianinazzi, 1983; Augé, 2001; Aroca et al., 2007). Hence, as long as mycorrhizal colonization is relatively uniformly distributed over the rooting system, the impact of mycorrhizae on the inverse SWIFT assessment can be resolved indirectly by altering k_R. However, inverse SWIFT may become prone to biased assessment when colonization is not uniform and the proportional contribution of water influx via mycorrhizae is substantial. Indeed, future endeavors to implement a more dynamic A_R and which can account for mycorrhizal colonization are encouraged.

Besides, many unknowns hamper model development. For instance, the extent to which fractionation during root water uptake or within the plant arises needs to be quantified before implementation. Here, root membrane (Lin and Sternberg, 1993; Zhao et al., 2016; Vargas et al., 2017) and mycorrhizal fractionation (Poca et al., 2019) present pathways that may introduce additional uncertainty. Also, stable water isotopes studies generally assume no alteration in δ_{xyl} once contained within the plant's conduit system. We encourage evaluation of this assumption, as δ_{xyl} enrichment via storage tissue or phloem is not unreasonable (Barbeta et al., 2020; Knighton et al., 2020), which would pose additional model interpretation complexities.

TABLE 2 | The standard error confidence intervals (i.e., 2.5 and 97.5 percentiles) and corresponding mean $\widehat{\beta}$ (±1SD) of inverse SWIFT simulated conditional density probability distributions, i.e., $P(\delta_{xyl}|\widehat{\beta}, \chi)$, of xylem water isotope composition of lianas and trees for Laussat, French Guiana.

	Growth form	Setup A Non-restricted		Setup B Restricted	
δ^2H	Liana	[−20.61; −0.42]	ns	[−7.78; −1.84]	*
	Tree	[−21.25; −4.15]		[−15.64; −9.22]	
$\delta^{18}O$	Liana	[−3.25; −0.65]	ns	[−1.64; −0.86]	*
	Tree	[−3.38; −1.17]		[−2.63; −1.86]	
$\widehat{\beta}$	Liana	0.792 ± 0.07	ns	0.657 ± 0.03	*
	Tree	0.901 ± 0.03		0.954 ± 0.04	

*Setups differ in considered restriction in soil water potential gradients (Ψ_S). Setup A: ignores restriction in Ψ_S. Setup B: improved characterization of Ψ_S. Parameterization of the inverse SWIFT procedure is provided in **Supplementary Table 3**. Significant (*) and non-significant (ns) differences are indicated.*

CONCLUSION

Root excavation can only provide a snapshot, a one-time-only measure due to its destructive nature. A stable water isotopes approach is advantageous for upscaling root attributes in space and time. Stable water isotope approaches can be applied over a wide range of edaphic and environmental conditions (Zhao et al., 2016). New developments in high temporal resolution monitoring of xylem water isotope composition would enable quantification of absorbing root surfaces distributions over time. This all can provide invaluable insights for understanding drought strategy and water competition among different plant species. However, this exciting prospect is only possible when techniques are unbiased under different edaphic or physiological conditions between plant species and sites. Our work here highlights a key role for mechanistic inverse plant model to help guide the research agenda for the critical zone and water stable isotope work.

DATA AVAILABILITY STATEMENT

The raw data supporting the conclusions of this article will be made available by the authors, upon reasonable request.

AUTHOR CONTRIBUTIONS

HV, MV, and PB supervised and provided guidance throughout all aspects of the research. HD, MV, and MD designed the study. PH-F provided guidance and training in sample collection, processing, and interpretation. HD collected the samples and data during the field campaign and performed the processing and analysis of the samples. HD, MV, MD, and FM developed and coded the model. All authors contributed to the interpretation of the results and to the text of the manuscript.

FUNDING

This research was funded by the European Research Council Starting Grant 637643 (TREECLIMBERS), the Carbon Mitigation Initiative at Princeton University (HD, MD, and MV), Agence Nationale de la Recherche "Investissement d'Avenir" grant (CEBA: ANR-10-LABX-25-01), the FWO grants (1214720N to FM and V401018N to HD), the Belgian American Educational Foundation (BAEF to HD and FM), and WBI to FM. The Programa de Formación de Personal Avanzado CONICYT, BECAS CHILE (PH-F) and the Commissie Wetenschappelijk Onderzoek (CWO, Faculty of Bioscience Engineering to PH-F).

ACKNOWLEDGMENTS

We thank Dries Van Der Heyden, Wim Van Nunen, Laurence Stalmans, Oscar Vercleyen, Katja Van Nieuland, Stijn Vandevoorde, and Clément Stahl for data collection and lab processing. We thank two reviewers and editor for their constructive comments on the manuscript. We are grateful to Cora N. Betsinger for proofreading and Kathy Steppe, Mathieu Javaux, Frank Sterck, Jan Van den Bulcke, and Stephen W. Pacala for insightful discussions.

SUPPLEMENTARY MATERIAL

The Supplementary Material for this article can be found online at: https://www.frontiersin.org/articles/10.3389/ffgc.2021.689335/full#supplementary-material

REFERENCES

Allison, G. B., Barnes, C. J., Hughes, M. W., and Leaney, F. W. J. (1983). Effect of climate and vegetation on oxygen-18 and deuterium profiles in soils. *Isotope Hydrol.* 105–123.

Araguás-Araguás, L., Rozanski, K., Gonfiantini, R., and Louvat, D. (1995). Isotope effects accompanying vacuum extraction of soil water for stable isotope analyses. *J. Hydrol.* 168, 159–171. doi: 10.1016/0022-1694(94)02636-p

Araguás-Araguás, L., Froehlich, K., and Rozanski, K. (1998). Stable isotope composition of precipitation over southeast Asia. *J. Geophys. Res.* 103, 28721–28742. doi: 10.1029/98jd02582

Aroca, R., Porcel, R., and Ruiz-Lozano, J. M. (2007). How does arbuscular mycorrhizal symbiosis regulate root hydraulic properties and plasma membrane aquaporins in Phaseolus vulgaris under drought, cold or salinity stresses? *N. Phytol.* 173, 808–816. doi: 10.1111/j.1469-8137.2006.01961.x

Augé, R. M. (2001). Water relations, drought and vesicular-arbuscular mycorrhizal symbiosis. *Mycorrhiza* 11, 3–42. doi: 10.1007/s005720100097

Baraloto, C., Rabaud, S., Molto, Q., Blanc, L., Fortunel, C., Herault, B., et al. (2011). Disentangling stand and environmental correlates of aboveground biomass in Amazonian forests. *Glob. Change Biol.* 17, 2677–2688. doi: 10.1111/j.1365-2486.2011.02432.x

Barbeta, A., Gimeno, T. E., Clavé, L., Fréjaville, B., Jones, S. P., Delvigne, C., et al. (2020). An explanation for the isotopic offset between soil and stem water in a temperate tree species. *N. Phytol.* 227, 766–779. doi: 10.1111/nph.16564

Barbeta, A., Jones, S. P., Clavé, L., Wingate, L., Gimeno, T. E., Fréjaville, B., et al. (2019). Unexplained hydrogen isotope offsets complicate the identification and quantification of tree water sources in a riparian forest. *Hydrol. Earth Syst. Sci.* 23, 2129–2146. doi: 10.5194/hess-23-2129-2019

Beyer, M., Hamutoko, J. T., Wanke, H., Gaj, M., and Koeniger, P. (2018). Examination of deep root water uptake using anomalies of soil water stable isotopes, depth-controlled isotopic labeling and mixing models. *J. Hydrol.* 566, 122–136. doi: 10.1016/j.jhydrol.2018.08.060

Böhm, W. (2012). *Methods of Studying Root Systems*. Netherland: Springer Science & Business Media.

Cabal, C., De Deurwaerder, H. P. T., and Matesanz, S. (2021). Field methods to study the spatial root density distribution of individual plants. *Plant Soil* 462, 1–19.

Carvalho, E. C. D., Martins, F. R., Oliveira, R. S., Soares, A. A., and Araújo, F. S. (2016). Why is liana abundance low in semiarid climates? *Austral. Ecol.* 41, 559–571. doi: 10.1111/aec.12345

Čermák, J., Ulrich, R., Staněk, Z., Koller, J., and Aubrecht, L. (2006). Electrical measurement of tree root absorbing surfaces by the earth impedance method: 2. Verification based on allometric relationships and root severing experiments. *Tree Physiol.* 26, 1113–1121. doi: 10.1093/treephys/26.9.1113

Chen, Y., Cao, K., Schnitzer, S. A., Fan, Z., Zhang, J., Bongers, F., et al. (2015). Water-use advantage for lianas over trees in tropical seasonal forests. *N. Phytol.* 205, 128–136. doi: 10.1111/nph.13036

Chen, Y., Helliker, B. R., Tang, X., Li, F., Zhou, Y., and Song, X. (2020). Stem water cryogenic extraction biases estimation in deuterium isotope composition of plant source water. *Proc. Natl. Acad. Sci. U. S. A.* 117, 33345–33350. doi: 10.1073/pnas.2014422117

Chen, Y., Schnitzer, S. A., Zhang, Y., Fan, Z., Goldstein, G., Tomlinson, K. W., et al. (2017). Physiological regulation and efficient xylem water transport regulate diurnal water and carbon balances of tropical lianas. *Funct. Ecol.* 31, 306–317. doi: 10.1111/1365-2435.12724

Clapp, R. B., and Hornberger, G. M. (1978). Empirical equations for some soil hydraulic properties. *Water Resour. Res.* 14, 601–604. doi: 10.1029/wr014i004p00601

Craig, H. (1961). Isotopic variations in meteoric waters. *Science* 133, 1702–1703. doi: 10.1126/science.133.3465.1702

Cristiano, P. M., Campanello, P. I., Bucci, S. J., Rodriguez, S. A., Lezcano, O. A., Scholz, F. G., et al. (2015). Evapotranspiration of subtropical forests and tree plantations: A comparative analysis at different temporal and spatial scales. *Agricult. Forest Meteorol.* 203, 96–106. doi: 10.1016/j.agrformet.2015.01.007

Dawson, T. E., and Ehleringer, J. R. (1991). Streamside trees that do not use stream water. *Nature* 350, 335–337. doi: 10.1038/350335a0

Dawson, T. E., Mambelli, S., Plamboeck, A. H., Templer, P. H., and Tu, K. P. (2002). Stable isotopes in plant ecology. *Annu. Rev. Ecol. Syst.* 33, 507–559.

De Deurwaerder, H., Hervé-Fernández, P., Stahl, C., Burban, B., Petronelli, P., Hoffman, B., et al. (2018). Liana and tree below-ground water competition—evidence for water resource partitioning during the dry season. *Tree Physiol.* 38, 1071–1083. doi: 10.1093/treephys/tpy002

De Deurwaerder, H. P. T., Visser, M. D., Detto, M., Boeckx, P., Meunier, F., Kuehnhammer, K., et al. (2020). Causes and consequences of pronounced variation in the isotope composition of plant xylem water. *Biogeosciences* 17, 4853–4870. doi: 10.5194/bg-17-4853-2020

Duong, T. (2007). ks: Kernel density estimation and kernel discriminant analysis for multivariate data in R. *J. Stat. Softw.* 21, 1–16.

Ehleringer, J. R., and Dawson, T. E. (1992). Water uptake by plants: perspectives from stable isotope composition. *Plant Cell Environ.* 15, 1073–1082. doi: 10.1111/j.1365-3040.1992.tb01657.x

FAO-ISRICI (1998). *World Reference Base for Soil Resources (WRB)*. FAO Rome: World Soil Resources.

Fogel, R. (1985). *Roots as primary producers in below-ground ecosystems*. FAO Rome: World Soil Resources.

Gaines, K. P., Meinzer, F. C., Duffy, C. J., Thomas, E. M., and Eissenstat, D. M. (2016). Rapid tree water transport and residence times in a Pennsylvania catchment. *Ecohydrology* 9, 1554–1565. doi: 10.1002/eco.1747

Gehring, C., Park, S., and Denich, M. (2004). Liana allometric biomass equations for Amazonian primary and secondary forest. *Forest Ecol. Manag.* 195, 69–83. doi: 10.1016/j.foreco.2004.02.054

Gerolamo, C. S., and Angyalossy, V. (2017). Wood anatomy and conductivity in lianas, shrubs and trees of Bignoniaceae. *IAWA J.* 38, 412–432. doi: 10.1163/22941932-20170177

Gerwing, J. J., Schnitzer, S. A., Burnham, R. J., Bongers, F., Chave, J., DeWalt, S. J., et al. (2006). A standard protocol for liana censuses. *Biotropica* 38, 256–261.

Gianinazzi-Pearson, V., and Gianinazzi, S. (1983). The physiology of vesicular-arbuscular mycorrhizal roots. *Plant Soil* 71, 197–209. doi: 10.1007/978-94-009-6833-2_20

Gibson, J. J., Birks, S. J., and Edwards, T. W. D. (2008). Global prediction of δA and δ2H-δ18O evaporation slopes for lakes and soil water accounting for seasonality. *Glob. Biogeochem. Cycles* 22:GB2031.

Gourlet-Fleury, S., Guehl, J. M., and Laroussinie, O. (2004). *Ecology and Management of a Neotropical Rainforest: Lessons Drawn From Paracou, a Long-Term Experimental Research Site in French Guiana*. New York: Elsevier.

Gröning, M. (2011). Improved water δ2H and δ18O calibration and calculation of measurement uncertainty using a simple software tool. *Rap. Commun. Mass Spectr.* 25, 2711–2720. doi: 10.1002/rcm.5074

Huang, C., Domec, J., Ward, E. J., Duman, T., Manoli, G., Parolari, A. J., et al. (2017). The effect of plant water storage on water fluxes within the coupled soil–plant system. *New Phytol.* 213, 1093–1106. doi: 10.1111/nph.14273

Iversen, C. M., Powell, A. S., McCormack, M. L., Blackwood, C. B., Freschet, G. T., Kattge, J., et al. (2018). *Fine-Root Ecology Database (FRED): A Global Collection of Root Trait Data with Coincident Site, Vegetation, Edaphic, and Climatic Data, Version 2*. Oak Ridge: Oak Ridge National Lab.(ORNL).

Jackson, R. B., Canadell, J., Ehleringer, J. R., Mooney, H. A., Sala, O. E., and Schulze. (1996). A global analysis of root distributions for terrestrial biomes. *Oecologia* 108, 389–411. doi: 10.1007/bf00333714

Javaux, M., Schröder, T., Vanderborght, J., and Vereecken, H. (2008). Use of a three-dimensional detailed modeling approach for predicting root water uptake. *Vadose Zone J.* 7, 1079–1088. doi: 10.2136/vzj2007.0115

Jobbagy, E. G., and Jackson, R. B. (2001). The distribution of soil nutrients with depth: Global patterns and the imprint of plants. *Biogeochemistry* 53, 51–77.

Johnson, D. M., Domec, J.-C., Woodruff, D. R., McCulloh, K. A., and Meinzer, F. C. (2013). Contrasting hydraulic strategies in two tropical lianas and their host trees. *Am. J. Bot.* 100, 374–383. doi: 10.3732/ajb.1200590

De Jong, van Lier, Q., Van Dam, J. C., Metselaar, K., De Jong, R., and Duijnisveld, W. H. M. (2008). Macroscopic root water uptake distribution using a matric flux potential approach. *Vadose Zone J.* 7, 1065–1078. doi: 10.2136/vzj2007.0083

Knighton, J., Kuppel, S., Smith, A., Soulsby, C., Sprenger, M., and Tetzlaff, D. (2020). Using isotopes to incorporate tree water storage and mixing dynamics into a distributed ecohydrologic modelling framework. *Ecohydrology* 13:e2201.

Leuschner, C., Coners, H., and Icke, R. (2004). In situ measurement of water absorption by fine roots of three temperate trees: species differences and differential activity of superficial and deep roots. *Tree Physiol.* 24, 1359–1367. doi: 10.1093/treephys/24.12.1359

Lin, G., and Sternberg, L. (1993). "Hydrogen isotopic fractionation by plant roots during water uptake in coastal wetland plants," in *Stable isotopes and plant carbon-water relations*, eds J. R. Ehleringer, A. E. Hall, and G. D. Farquhar (Netherland: Elsevier), 497–510. doi: 10.1016/b978-0-08-091801-3.50041-6

Magh, R.-K., Eiferle, C., Burzlaff, T., Dannenmann, M., Rennenberg, H., and Dubbert, M. (2020). Competition for water rather than facilitation in mixed beech-fir forests after drying-wetting cycle. *J. Hydrol.* 587:124944. doi: 10.1016/j.jhydrol.2020.124944

Marshall, J. D., Cuntz, M., Beyer, M., Dubbert, M., and Kuehnhammer, K. (2020). Borehole equilibration: testing a new method to monitor the isotopic composition of tree xylem water in situ. *Front. Plant Sci.* 11:358. doi: 10.3389/fpls.2020.00358

Martin-Gomez, P., Barbeta, A., Voltas, J., Penuelas, J., Dennis, K., Palacio, S., et al. (2015). Isotope-ratio infrared spectroscopy: a reliable tool for the investigation of plant-water sources? *N. Phytol.* 207, 914–927. doi: 10.1111/nph.13376

Meinzer, F. C., Brooks, J. R., Domec, J., Gartner, B. L., Warren, J. M., Woodruff, D. R., et al. (2006). Dynamics of water transport and storage in conifers studied with deuterium and heat tracing techniques. *Plant Cell Environ.* 29, 105–114. doi: 10.1111/j.1365-3040.2005.01404.x

Meinzer, F. C., Goldstein, G., and Andrade, J. L. (2001). Regulation of water flux through tropical forest canopy trees: do universal rules apply? *Tree Physiol.* 21, 19–26. doi: 10.1093/treephys/21.1.19

Meißner, M., Köhler, M., Schwendenmann, L., and Hölscher, D. (2012). Partitioning of soil water among canopy trees during a soil desiccation period in a temperate mixed forest. *Biogeosciences* 9, 3465–3474. doi: 10.5194/bg-9-3465-2012

Mennekes, D., Rinderer, M., Seeger, S., and Orlowski, N. (2021). Ecohydrological travel times derived from in situ stable water isotope measurements in trees during a semi–controlled pot experiment. *Hydrol. Earth Syst. Sci. Discuss.* 2021, 1–34. doi: 10.1046/j.1440-1703.1998.00240.x

Ogle, K., Wolpert, R. L., and Reynolds, J. F. (2004). Reconstructing plant root area and water uptake profiles. *Ecology* 85, 1967–1978. doi: 10.1890/03-0346

Orlowski, N., Frede, H. G., Brüggemann, N., and Breuer, L. (2013). Validation and application of a cryogenic vacuum extraction system for soil and plant water extraction for isotope analysis. *J. Sens. Sens. Syst.* 2, 179–193. doi: 10.5194/jsss-2-179-2013

Penna, D., Hopp, L., Scandellari, F., Allen, S. T., Benettin, P., Beyer, M., et al. (2018). Ideas and perspectives: Tracing terrestrial ecosystem water fluxes using hydrogen and oxygen stable isotopes–challenges and opportunities from an interdisciplinary perspective. *Biogeosciences* 15, 6399–6415. doi: 10.5194/bg-15-6399-2018

Phillips, D. L., and Gregg, J. W. (2003). Source partitioning using stable isotopes: coping with too many sources. *Oecologia* 136, 261–269. doi: 10.1007/s00442-003-1218-3

Poca, M., Coomans, O., Urcelay, C., Zeballos, S. R., Bodé, S., and Boeckx, P. (2019). Isotope fractionation during root water uptake by Acacia caven is enhanced by arbuscular mycorrhizas. *Plant Soil* 441, 1–13.

Preston, R. J. (1942). The growth and development of the root systems of juvenile lodgepole pine. *Ecol. Monogr.* 12, 449–468. doi: 10.2307/1943040

R Core Team (2017). *R: A Language and Environment for Statistical Computing*. R Foundation for Statistical Computing. Vienna: R Core Team.

Rothfuss, Y., and Javaux, M. (2017). Reviews and syntheses: Isotopic approaches to quantify root water uptake: a review and comparison of methods. *Biogeosciences* 14:2199. doi: 10.5194/bg-14-2199-2017

Rozanski, K., Araguás-Araguás, L., and Gonfiantini, R. (1993). Isotopic patterns in modern global precipitation. *Clim. Change Cont. Isot. Rec.* 1993, 1–36. doi: 10.1029/gm078p0001

Rüdinger, M., Hallgren, S. W., Steudle, E., and Schulze, E.-D. (1994). Hydraulic and osmotic properties of spruce roots. *J. Exp. Bot.* 45, 1413–1425. doi: 10.1093/jxb/45.10.1413

Ruth, B., Khalvati, M., and Schmidhalter, U. (2011). Quantification of mycorrhizal water uptake via high-resolution on-line water content sensors. *Plant Soil* 342, 459–468. doi: 10.1007/s11104-010-0709-3

Sands, R., Fiscus, E. L., and Reid, C. P. P. (1982). Hydraulic properties of pine and bean roots with varying degrees of suberization, vascular differentiation and mycorrhizal infection. *Funct. Plant Biol.* 9, 559–569. doi: 10.1071/pp9820559

Seeger, S., and Weiler, M. (2021). Temporal dynamics of tree xylem water isotopes: In-situ monitoring and modelling. *Biogeosciences Discuss.* 2021, 1–41.

Smith-Martin, C. M., Bastos, C. L., Lopez, O. R., Powers, J. S., and Schnitzer, S. A. (2019). Effects of dry-season irrigation on leaf physiology and biomass allocation in tropical lianas and trees. *Ecology* 100:e02827.

Smith-Martin, C. M., Xu, X., Medvigy, D., Schnitzer, S. A., and Powers, J. S. (2020). Allometric scaling laws linking biomass and rooting depth vary across ontogeny and functional groups in tropical dry forest lianas and trees. *New Phytol.* 226, 714–726. doi: 10.1111/nph.16275

Soethe, N., Lehmann, J., and Engels, C. (2006). The vertical pattern of rooting and nutrient uptake at different altitudes of a south Ecuadorian montane forest. *Plant Soil* 286, 287–299. doi: 10.1007/s11104-006-9044-0

Steudle, E., and Meshcheryakov, A. B. (1996). Hydraulic and osmotic properties of oak roots. *J. Exp. Bot.* 47, 387–401. doi: 10.1093/jxb/47.3.387

Vargas, A. I., Schaffer, B., Yuhong, L., Sternberg, L., and da, S. L. (2017). Testing plant use of mobile vs immobile soil water sources using stable isotope experiments. *New Phytol.* 215, 582–594. doi: 10.1111/nph.14616

Vogel, T., Dohnal, M., Dusek, J., Votrubova, J., and Tesar, M. (2013). Macroscopic modeling of plant water uptake in a forest stand involving root-mediated soil water redistribution. *Vadose Zone J.* 12, 1–12.

von Freyberg, J., Allen, S. T., Grossiord, C., and Dawson, T. E. (2020). Plant and root-zone water isotopes are difficult to measure, explain, and predict: Some practical recommendations for determining plant water sources. *Methods Ecol. Evolut.* 11, 1352–1367. doi: 10.1111/2041-210x.13461

Walker, C. D., and Richardson, S. B. (1991). The use of stable isotopes of water in characterizing the source of water in vegetation. *Chem. Geol.* 94, 145–158. doi: 10.1016/0168-9622(91)90007-j

Wershaw, R. L., Friedman, I., Heller, S. J., and Frank, P. A. (1966). Hydrogen isotopic fractionation of water passing through trees. *Adv. Organic Geochem.* 118, 55–67. doi: 10.1016/b978-0-08-012758-3.50007-4

White, J. W. C., Cook, E. R., Lawrence, J. R., and Broecker, W. S. (1985). The D/H ratios of sap in trees - implications for water sources and tree-ring D/H ratios. *Geochim. Cosmochim. Acta* 49, 237–246. doi: 10.1016/0016-7037(85)90207-8

Wu, L., McGechan, M. B., McRoberts, N., Baddeley, J. A., and Watson, C. A. (2007). SPACSYS: integration of a 3D root architecture component to carbon, nitrogen and water cycling—model description. *Ecol. Model.* 200, 343–359. doi: 10.1016/j.ecolmodel.2006.08.010

Zanne, A. E., Westoby, M., Falster, D. S., Ackerly, D. D., Loarie, S. R., Arnold, S. E. J., et al. (2010). Angiosperm wood structure: global patterns in vessel anatomy and their relation to wood density and potential conductivity. *Am. J. Bot.* 97, 207–215. doi: 10.3732/ajb.0900178

Zhao, L., Wang, L., Cernusak, L. A., Liu, X., Xiao, H., Zhou, M., et al. (2016). Significant difference in hydrogen isotope composition between xylem and tissue water in Populus euphratica. *Plant Cell Environ.* 39, 1848–1857. doi: 10.1111/pce.12753

Zimmermann, U., Ehhalt, D., and Münnich, K. (1967). "Soil-Water movement and evapotranspiration: changes in the isotopic composition of the water," in *Conference on Isotopes in Hydrology*, (Vienna: WHO), 567–585.

Conflict of Interest: The authors declare that the research was conducted in the absence of any commercial or financial relationships that could be construed as a potential conflict of interest.